Hydrothermal Synthesis: Low–Temperature Subcritical Water for Ceria–Zirconia Mixed Oxides Preparation

Siti Machmudah[1,*], Widiyastuti[1], Wahyudiono[2], Sugeng Winardi[1], Hideki Kanda[2], and Motonobu Goto[2]

[1]*Department of Chemical Engineering, Faculty of Industrial Technology, Institut Teknologi Sepuluh Nopember, Surabaya 60111, Indonesia*

[2]*Department of Materials Process Engineering, Graduate School of Engineering, Nagoya University, Nagoya 464–8603, Japan*

* ***Corresponding author:***

email: machmudah@chem-eng.its.ac.id

Received: July 5, 2019
Accepted: April 14, 2020

DOI: 10.22146/ijc.47357

Abstract: *A low-temperature hydrothermal synthesis technique was employed as a medium to produce ceria–zirconia mixed oxides particles at temperatures of 200–300 °C and pressure of 10 MPa in a batch process. At these conditions, the average crystallite sizes of ceria–zirconia mixed oxides increased slightly with increasing reaction temperature when the feed solution containing ceria and zirconia with a ratio of 1:1 was fed. SEM images illustrated that the morphologies of the ceria–zirconia mixed oxides particles were spherical and spherical–like with a diameter of around 100 nm. The EDX spectrum indicated that the signal corresponding to the ceria and the zirconia elements at 5 and 2 keV, respectively, were strongly detected in the products. The XRD pattern revealed that the mixed metal oxides particle products that comprised of cerium and zirconium oxides particles with cubic and monoclinic structures, respectively, were affected by their molar content in the feed solution.*

Keywords: *ceria–zirconia oxides; metal oxides; hydrothermal; subcritical; synthesis*

■ INTRODUCTION

Ceria–based materials have been known as one of the most attractive materials for environmental and energy applications due to their distinct defect chemistry. From an environmental point of view, ceria has been used as a key component in composite catalysts due to how relatively easy it can change between its two stable oxidation states This cerium(IV) oxide–cerium(III) oxide cycle activity allows switching from cerium(IV) oxide under oxidizing conditions to cerium(III) oxide under net declining conditions and vice versa. The highly mobile oxygen vacancies in high concentrations of cerium may promote the rapid change of the oxidation state and may result in its ability to store and release oxygen. This phenomenon resulted in beneficial effects and was an important factor for its catalytic activity [1-4]. Regarding energy applications, ceria–based materials have been known to have the highest ionic and electronic conductivity by reducing the partial pressure of oxygen at environment temperatures below 1000 °C [5].

Despite the fact that cerium oxide is an attractive rare earth oxide and has been widely investigated for many applications, the sintering of this oxide can occur at high temperatures (over 1000 °C) via a redox reaction. This sintering process may decrease the catalytic activity and the capacity of oxygen storage and release significantly [6-7]. To avoid the effect of the sintering process when cerium oxide is employed at high temperatures, it is very important to stabilize the cerium oxide by addition or modification using different elements. In the current study, cerium oxide is modified by adding zirconium oxide and prepared by hydrothermal treatment in a batch process. Zirconia (zirconium dioxide, ZrO_2) possesses several unique properties that have proven to be superior to other ceramic elements. It is known to be able to improve morphological and redox stability at high temperatures.

Zirconia has good mechanical strength, good resistance against crack propagation, good thermal resistance, relatively high thermal expansion coefficient, and low thermal conductivity at high temperatures (over 1000 °C) [8-11]. Due to these properties, zirconia was used in many industrial applications as ceramic bodies and was also used as reinforcement in various composite materials to improve their mechanical properties.

It is widely known that ceramic nanoparticles can be prepared and synthesized by various approaches. In general, the applied techniques for the synthesis of ceramic nanoparticles can be classified into two types of techniques: chemical and physical [12]. Each technique possesses its own advantages and disadvantages; however, whichever technique is applied, it is important to focus on attaining monodispersity or long–term stability of the particle products. In this work, the hydrothermal synthesis technique, as one of the wet–chemical synthesis techniques, was employed as a media to generate ceria–zirconia mixed oxides nanoparticles from cerium and zirconium oxides. This technique is inexpensive and less hazardous, therefore environmentally friendly, and only requires the use of simple equipment. The hydrothermal synthesis technique can be referred to as crystal growth or heterogeneous crystal synthesis in the presence of aqueous media or mineralizers under high temperature and pressure conditions from materials that are insoluble under ordinary conditions (< 100 °C, < 1 atm) [13].

Regarding ceramic particle generation, the hydrothermal synthesis technique has several advantages, such as how the size and morphology of the particle products are easily managed by varying the synthesis conditions. Allowing the generation of materials with an elemental oxidation state, the synthesis process can be directly applied to many materials to produce the desired crystalline phase at low operating temperatures [14-15]. Furthermore, it is important to judge the conditions of hydrothermal synthesis with water media. In this case, subcritical synthesis conditions would be applied as a media for the synthesis process, where the temperature of the water is increased to above its boiling point (between 100 and 374 °C). However, the pressure is required to be tuned to maintain water in its liquid form. Under these conditions, the physical and chemical properties of water change quite dramatically, including the ionic product (K_w), density, and dielectric constant of water. Hence, water at subcritical conditions gives a favorable reaction medium for particle generation, owing to the promoted reaction rate. According to the nucleation theory, the high degree of supersaturation is caused by declined solubility [13-16].

■ EXPERIMENTAL SECTION

Materials

The commercial cerium(III) nitrate hexahydrate ($Ce(NO_3)_3{\cdot}6H_2O$, product no. 035–09735) and zirconium nitrate oxide dehydrate ($ZrO(NO_3)_2{\cdot}2H_2O$, product no. 265–00915) were used as starting materials. They were purchased from Wako Pure Chemical Industries Ltd. (Japan), with purities of more than 97.0%. Nitrogen gas obtained from Samator PT (Gresik, Indonesia) was used to purge air during experimental preparation. During preparation, the cerium or zirconium solution was prepared by dissolving cerium(III) nitrate hexahydrate or zirconium nitrate oxide dehydrate in a flask with deionized water. The concentration of each specimen was 0.06 M.

Instrumentation

The experiments were performed in batch type reactors made of SUS–316 and comprised of a tube body and cap (AKICO Co. Ltd., Japan; 8.8 mL). This reactor was operated at 300 °C and 35 MPa. The electric furnace (Linn High Therm GmbH, model VMK 1600, Germany) was used to heat the reactors. The particle products were characterized using a scanning electron microscope (SEM, JEOL JSM–6390LV, Japan), particle size analysis (PSA, a Malvern Zetasizer nanoseries, Germany), energy dispersive X–ray (EDX) spectroscopy equipped in a Zeiss EVO MA 10 scanning electron microscope (SEM) from Bruker, thermogravimeter (TG–50, Shimadzu, Japan), and BET (Brunauer–Emmett–Teller, Nova 1200, Quantachrome, USA).

Procedure

An aqueous solution containing zirconium and cerium substances with different molar ratios was loaded

into the reactor and sealed tightly. The given amounts of solution corresponded to 0.71–0.87 g mL^{-3} water density. Before closing the reactor, nitrogen gas was introduced to the reactor to purge the air. Next, the reactor was put in the electric furnace and quickly heated to 200–300 °C. The temperature in the reactor was determined by a thermocouple (K–type), and the pressure was determined from the water densities. After 2 h (including the heating time of about 15 min) [13], the reactor was taken out from the electric furnace and quickly quenched in a water bath at room temperature. The collected products were dried and calcined. Fig. 1 shows the general process of the particle synthesis by hydrothermal technique.

The morphologies of the calcined powder products were observed using a scanning electron microscope after gold coating. The size was determined by using particle size analysis (PSA). The elemental analysis of the particle products was investigated by using energy dispersive X–ray (EDX) spectroscopy, which was equipped in a Zeiss EVO MA 10 scanning electron microscope (SEM). X–ray diffraction (XRD) patterns were employed to confirm that the crystal structure of ceria–zirconia was generated through this hydrothermal synthesis method. The capacity of oxygen storage of the ceria–zirconia particle product was determined by using a thermogravimeter [17-18]. The surface area of the ceria–zirconia particle products was determined by using the BET method.

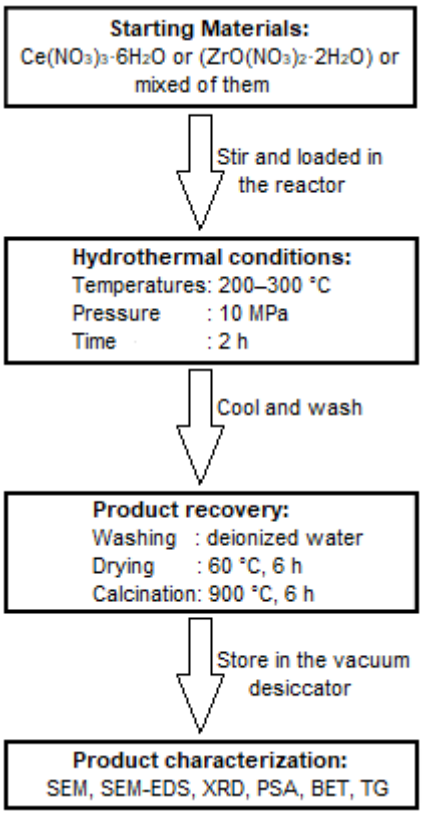

Fig 1. Flowchart summary of the hydrothermal synthesis

■ RESULTS AND DISCUSSION

Fig. 2 and 3 show the typical SEM images of synthesized particles from cerium or zirconium solution under hydrothermal conditions at various operating temperatures with 2 h synthesis time. These results reveal that ceria or zirconia particles can be produced easily in water at the applied reaction temperatures. At subcritical conditions, the water turns into a solvent with weak polarity and possesses both acidic and basic properties. These beneficial properties may result in faster and easier particle generation via synthesis reaction. The water molecules underwent dissociation into H^+ and OH^-, which were illustrated as ion products. These ion products rose as the environmental temperature was increased and achieved the highest value when the environment temperature was around 300 °C. Simultaneously, the dielectric constant of water also changed. At ordinary conditions, the dielectric constant of water is around 78; thus, water becomes favorable to dissolve the inorganic salts.

When the environment temperature was increased to 200 or 300 °C, the values of the water dielectric constants decreased to 35 or 21. This means that water was still favored to dissolve non–polar organic compounds and to serve a homogenous phase for reactions. The solubility of ionic inorganic salts became lower and was able to promote the solute precipitation to generate fine particles via hydrolysis reaction. At the same time, the change of water properties (acid–base characters) can enhance inorganic salts hydrolysis to obtain hydroxides without the presence of catalysts [13,15-16,19]. Therefore, based on benefits such as the reaction rate enhancement and the reduction of solubility that causes a high degree of supersaturation, subcritical water conditions serve as a comfortable reaction media for particle generation.

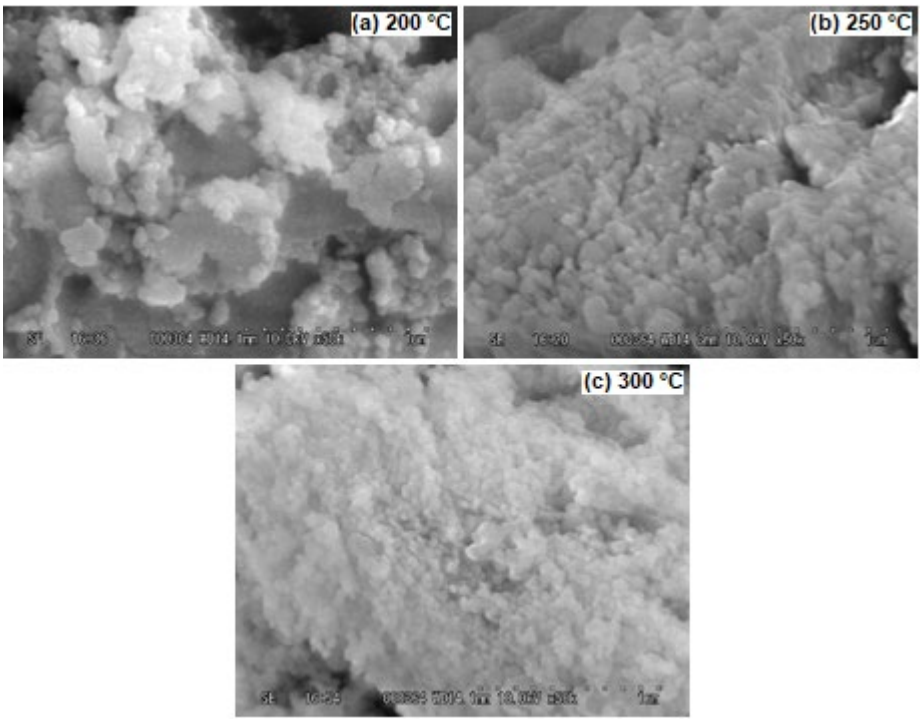

Fig 2. SEM images of ceria particle products

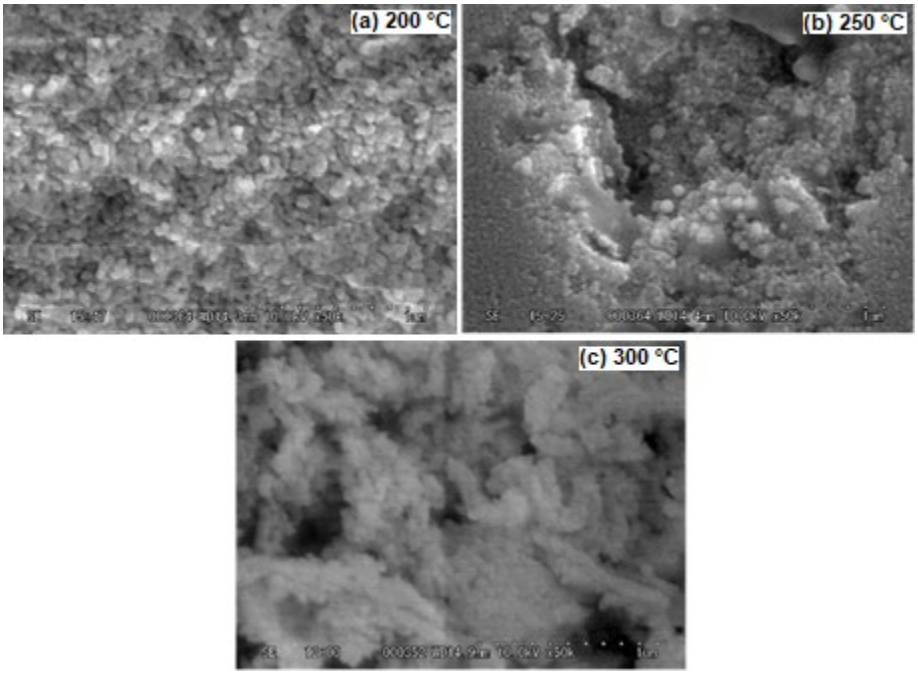

Fig 3. SEM images of zirconia particle products

Adschiri et al. [20] reported that there were two reaction steps for particle generation in hydrothermal conditions from inorganics salts as starting materials, namely, hydrolysis and dehydration reaction. In brief, the metal salt in the aqueous solution was hydrolyzed into metal hydroxide. Next, the precipitation of metal oxide crystals in nano– or micro–sized particles from solution occurs via dehydration reaction to form particle products.

The formation mechanism of metal oxide particles from the metal nitrate solution was as follows [20-21]:

Hydrolysis

$$M(NO_3)_{x(1)} + xH_2O_{(1)} \rightarrow M(OH)_{x(s)} + xHNO_{3(1)} \quad (1)$$

Dehydration

$$M(OH)_{x(s)} \rightarrow MO_{x/2(s)} + (x/2)H_2O_{(1)} \quad (2)$$

where M is a metal.

As displayed in Fig. 2 and 3, most of the generated ceria and zirconia particles appeared to have spherical morphologies with a diameter of less than 100 nm. The reason for these results may be due to the good solubility of cerium(III) nitrate hexahydrate, and zirconium nitrate oxide dehydrate in aqueous media, while the nitrate component from the starting materials may have prevailed as a surfactant to promote the generation of micelles. Similar to other anions that are employed as a coprecipitator, nitrate anions and water are able to surround the surface of cerium or zirconium, which would lead to the generation of fine particles. Due to this phenomenon, the shapes of the generated metal oxide particles, including ceria and zirconia, seemed to have spherical or spherical–like morphologies when the synthesis reaction was carried out in hydrothermal conditions [21-24].

The morphologies of the samples did not shift with the increase in operating temperatures and reaction time. This indicated that the different crystallographic planes of ceria or zirconia particles might have a similar growth rate at these conditions. As a result, the ceria or zirconia particle products that were generated at different temperatures or different reaction times had similar morphology. The results also indicated that hydrothermal reaction conditions are convenient and enough to initiate the formation of fine particles from cerium nitrate or zirconium nitrate solution through hydrolysis and dehydration reactions. Hayashi and Hakuta [13] reported that the hydrothermal synthesis technique involves heterogeneous particle synthesis or particle growth in the existence of liquid media under temperatures (below 300 °C) high enough to start chemical reactions for several hours (h). Afterwards, the hydrothermal synthesis technique for the generation of ceria–zirconia mixed oxides nanoparticles was set at 2 h reaction time.

Fig. 4 shows the XRD spectra of (a) ceria and (b) zirconia particles obtained by hydrothermal synthesis when the experiments were performed at 300 °C with a reaction time of 2 h. XRD has been applied and mainly relied on for the identification of monoclinic, tetragonal, and cubic phases in materials [25-26]. As shown in Fig. 4(a), the diffraction peaks at 28.5, 33.2, 47.4, 56.5, 59.0, and 69.5° were found clearly on the XRD pattern of the ceria particle products, and can be attributed to the (111), (200), (220), (311), (222), and (400) crystalline faces (JCPDS ICDD PDF card 00–043–1002), respectively. These features revealed that the ceria particle products seemed to have a cubic fluorite–type structure [27-29], where each cerium atom was surrounded by eight oxygen atoms in a face–centered cubic order. This cubic fluorite structure is stable from room temperature to its melting point at around 2400 °C. In addition, ceria particles are also known to be generated by the hydrothermal synthesis method at low operating temperatures.

Tok et al. [27] conducted an experiment for ceria nanocrystalline particles by using a hydrothermal synthesis method at low operating temperatures. They found that ceria particle products containing cubic–fluorite structures were easily generated with relatively good crystallinity at a temperature of around 250 °C. They also reported that increasing the reaction time did not give influence to the properties of the ceria particle products. A similar result was also found when the zirconia particle products were subjected to the X–ray diffraction device (see Fig. 4(b)). The monoclinic, tetragonal, and cubic structures were found in the zirconia particle products; however, the monoclinic structure was found dominantly in the zirconia particle products compared to tetragonal or cubic structures. Hence, the X–ray diffraction patterns for tetragonal or cubic structures were not presented.

The same results were found when Machmudah et al. [15] conducted experiments for hydrothermal synthesis to produce zirconia particles at temperatures of 200–300 °C. They explained that the zirconia particle

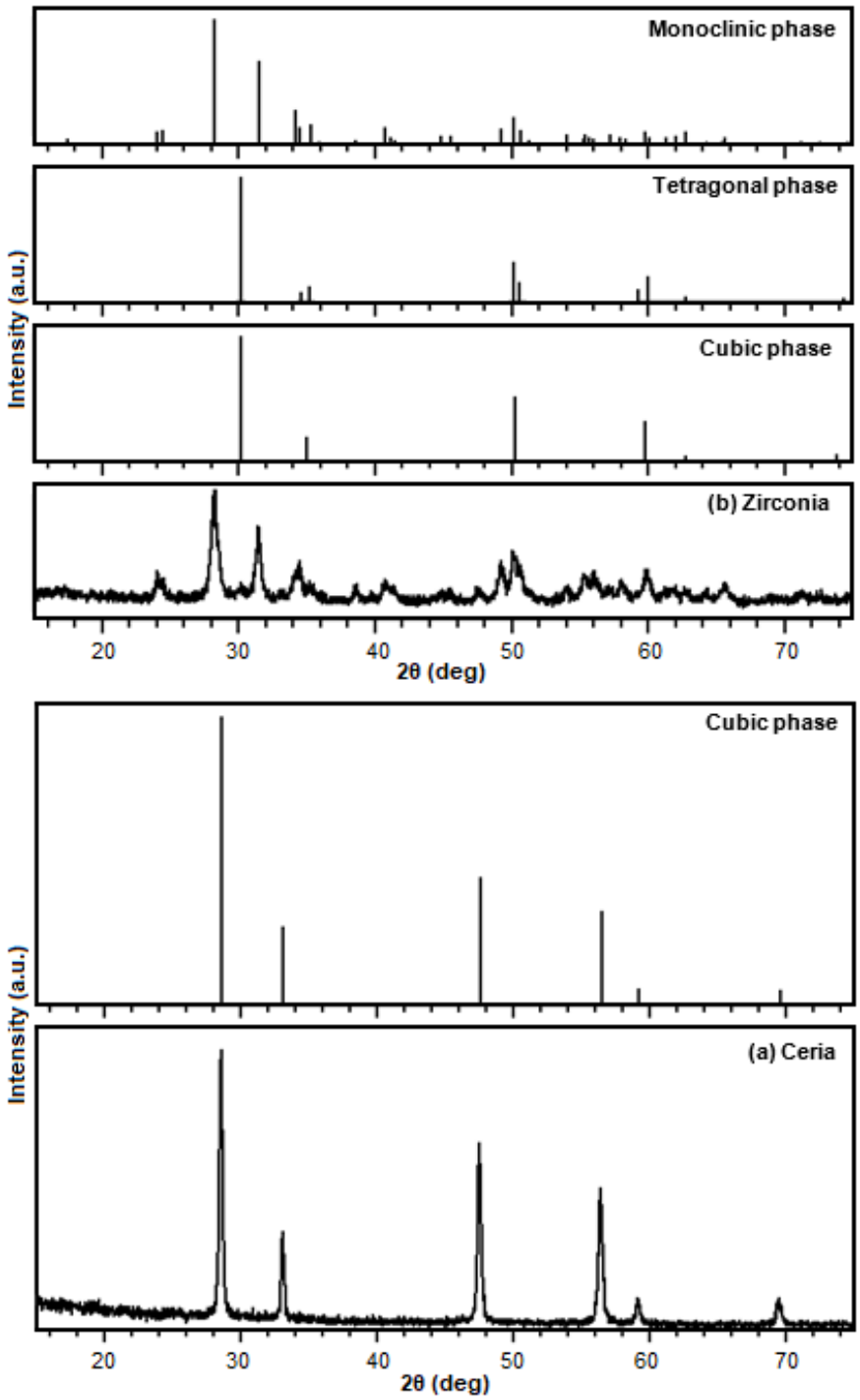

Fig 4. X–ray diffraction spectra of (a) ceria and (b) zirconia particles

products with the monoclinic structure were generated through a dissolution or precipitation process followed by the formation of the tetragonal and cubic structures under subcritical water conditions. As a result, the hydrothermal synthesis products from the zirconium nitrate solution via the hydrolysis and the dehydration reactions under subcritical water conditions would predominantly be monoclinic zirconia particles. Thus, it can be concluded that the ceria particles with a cubic fluorite–type structure and the monoclinic zirconia particles were

successfully generated from cerium nitrate and zirconium nitrate solutions under hydrothermal conditions.

Fig. 5 shows the typical SEM images and XRD spectra of synthesized particle products from ceria–zirconia solution in a 1:1 ratio at various reaction temperatures with 2 h reaction time. Similar to the pure ceria or pure zirconia particle products, the collected particle products from ceria–zirconia mixed oxides solution seemed to have spherical or spherical–like (oval) shapes at every reaction temperature. Apparently, at these ranges of temperature, the shapes of the ceria–zirconia particles were dominantly affected by the composition of feed solution that was loaded in the SUS reactor [30-34].

Phokha et al. [30] conducted experiments for the production of monodisperse ceria particles in nano–sphere shapes under hydrothermal conditions. They reported that the feed composition containing cerium nitrate as a cerium source had a significant influence on the morphology of the final product. They also found that the cerium source from cerium nitrate is most favorable

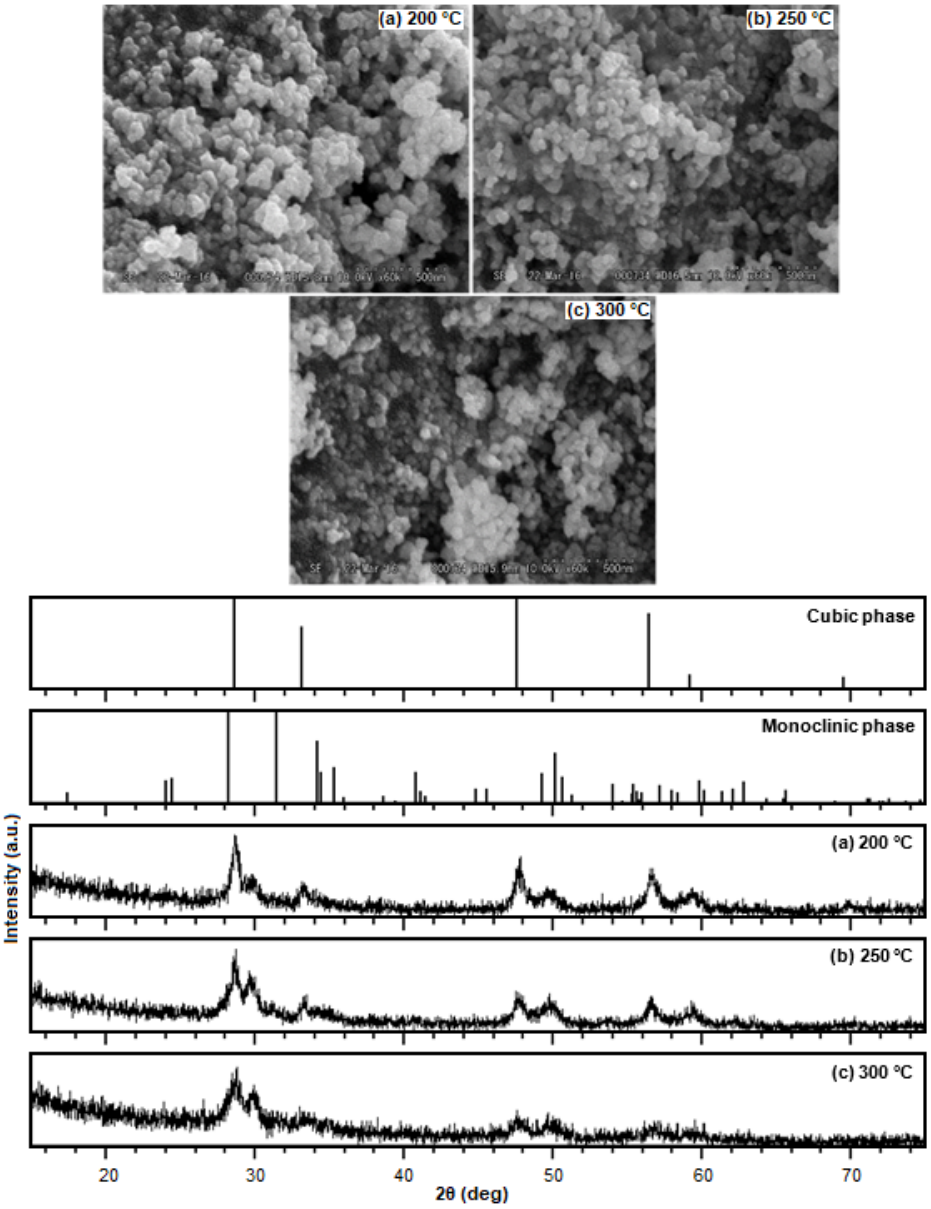

Fig 5. SEM images and X–ray diffraction spectra of ceria–zirconia particle products with 1:1 ratio at various reaction temperatures

for the generation of ceria particles with spherical or spherical–like shapes. Zhang et al. [32] also found the spherical or spherical–like shapes of ceria–zirconia particles when they performed the hydrothermal synthesis of ceria–zirconia nanocomposites from a feed solution containing cerium(III) nitrate hexahydrate and zirconium nitrate hexahydrate. Furthermore, they also reported that the morphologies of the ceria–zirconia nanocomposites did not shift after the calcination process.

When the particles produced from a feed solution containing cerium and zirconium were submitted into the XRD apparatus, the peaks of ceria and zirconia were detected clearly in the XRD patterns at each reaction temperature. Although the hydroxylation of metal ions, including cerium and zirconium, can be significantly stimulated by elevating the reaction temperature at hydrothermal conditions, the characteristic peaks of ceria–zirconia did not seem to shift with increasing reaction temperature. It is well known that the hydrolysis reaction may facilitate and promote complex precursor generation to metal oxide nucleation at hydrothermal conditions (200–300 °C) [13].

Hayashi and Hakuta [13] proposed the mechanism of metal oxide particle generation from metal nitrate solution under hydrothermal conditions. In brief, the hydrated metal ions were hydrolyzed to metal hydroxide. In the next step, the metal hydroxides proceeded to precipitate as metal oxides via dehydration reaction. Due to this phenomenon, the size of the metal oxide particle products was strongly affected by the rate of hydrolysis and the metal oxide solubility in the solvent media. In this work, by using the Scherrer equation, the average crystallite size of ceria–zirconia particle products was estimated from the diffraction peak width at half the peak height (full width half maximum, FWHM). Approximately, the average crystallite sizes of ceria–zirconia particle products at 200, 250, and 300 °C were 7.9, 8.54, and 10.12 nm, respectively. It seemed that the average crystallite sizes slightly increased with the increase in reaction temperature.

In order to accomplish the ceria–zirconia particle analysis, the characterization of the particle products was also carried out by using energy dispersive X–ray (EDX) analysis, which was attached to the SEM apparatus system. This analysis technique is the general type of X–ray spectroscopy that is simple, non–destructive, and applicable to a small amount of sample. As presented in Fig. 6, the EDX spectrum describes a strong signal corresponding to the ceria and the zirconia elemental regions at around 5 and 2 keV, respectively [35-36]. The peaks that correspond to the existence of ceria and zirconia elements were also found in the regions around 0.2 and 0.9 keV, respectively. It seemed that the ceria and the zirconia elements were a major component compared to oxygen. This is, of course, good news in terms of ceria–zirconia particles formation from cerium(III) nitrate hexahydrate and zirconium nitrate hexahydrate solutions.

The oxygen might have originated from the solvent and/reactants that were bound to the surface of the ceria–zirconia particles. A similar spectrum was also obtained when the ceria–zirconia particles generated from the 200 and 300 °C reaction temperatures were submitted to the EDX device system. Thus, the EDX data for these mixed metal oxide products after hydrothermal treatment at temperatures of 200 and 300 °C are not presented. Judging the results, it can be concluded that the formation of ceria–zirconia particles from the feed solution containing cerium and zirconium elements were successfully performed under hydrothermal conditions at temperatures of 200–300 °C.

Fig. 7 shows the XRD patterns for a series of ceria–zirconia products obtained via hydrothermal reactions at a temperature of 250 °C and 2 h of reaction time with varying molar ratios. As explained above, the composition of the feed solution has an extraordinary influence on the nature and properties of the mixed oxides particles. Proportionally, when cubic fluorite ceria oxides and monoclinic zirconia oxides (see Fig. 4) was fed as the starting materials to produce particles via hydrothermal process, the precipitated particle products with a similar composition to the feed solution can be obtained.

As shown in Fig. 7, when the molar content of ceria oxide in the feed solution was over 50%, the particle products seemed to have a cubic structure. Otherwise, they

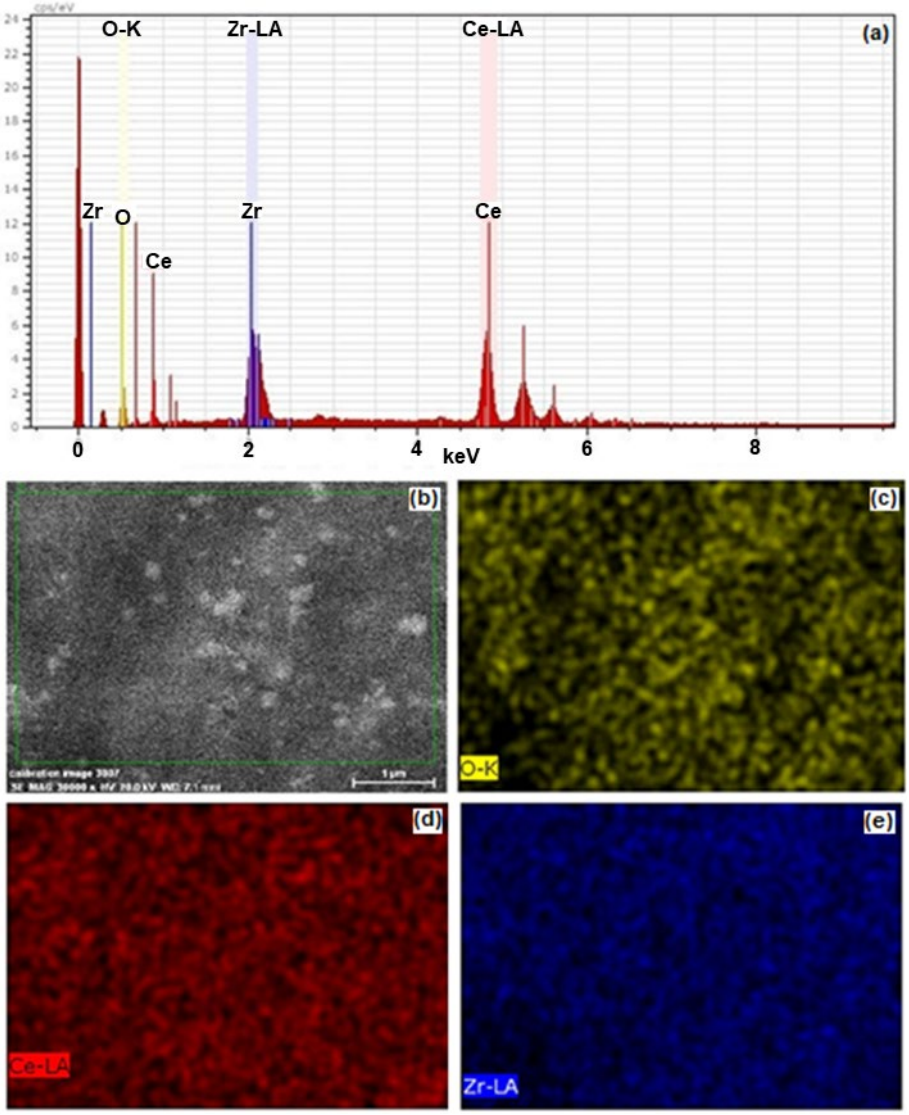

Fig 6. EDX spectrum (a) and dark–field SEM image of ceria–zirconia particles (b) with the corresponding EDX maps for oxygen (c), ceria (d), and zirconia (e) elements (reaction temperature: 250 °C; ceria–zirconia ratio: 1:1; time: 2 h)

appeared as monoclinic structures the same as that of zirconia. The zirconia phase intensity was very weak when the feed solution ratio of ceria to zirconia was 2:1 and 4:1. This result was in agreement with the low amounts of zirconia in the feed solution (ceria–rich feed solution). By increasing the content of zirconia in the starting materials, gradually the shifting of the diffraction lines at 111, 220, and 311, that are attributed to the cubic fluorite–type structure of ceria, was observed [29,37]. Other than that, there were no other diffraction peaks on the XRD patterns of the mixed ceria–zirconia particle products.

It can be assumed that the structure of the ceria–zirconia particle products had uniform distribution. When these particle products were submitted in the particle size analysis (PSA) device, the diameter size of the particles was found at around 100 nm. Note that the particle size distribution was not determined during this study due to the limitation of the analytical equipment. On average, the mean diameter size of the particles was observed at around 99, 125, 92, 118, and 116 nm when the ceria to zirconia ratios of the feed solution was 4:1, 2:1, 1:1, 1:2, and 1:4, respectively. However, by using the Scherrer equation, the estimated

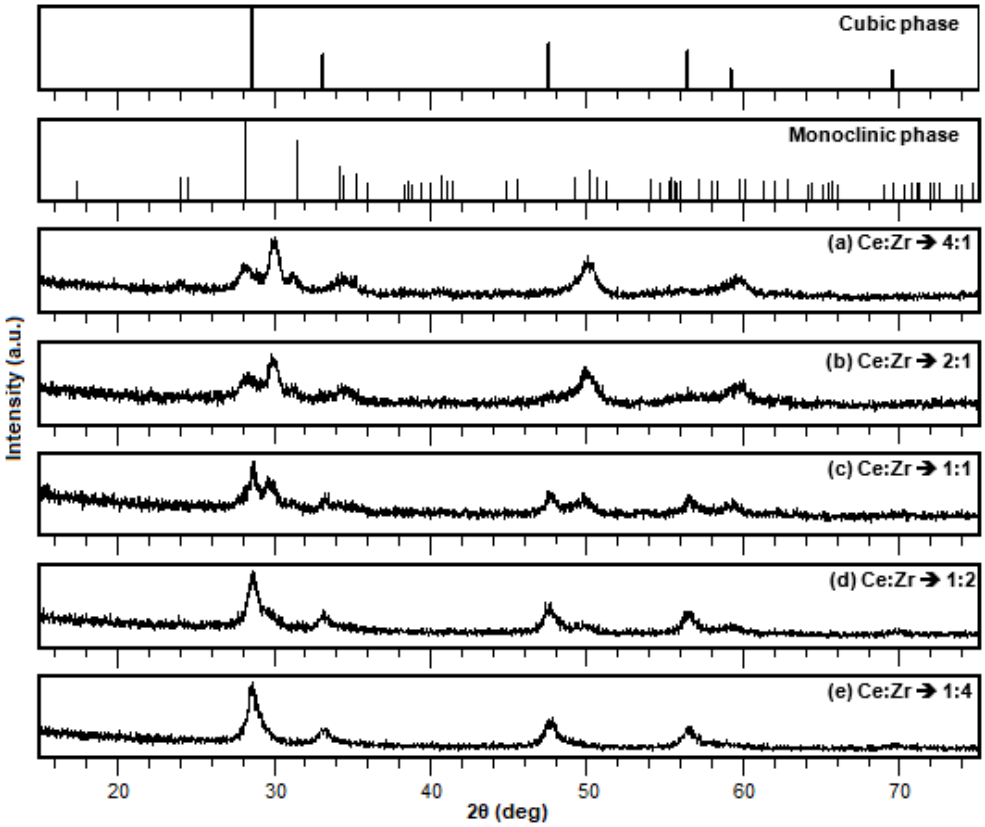

Fig 7. X–ray diffraction spectra of ceria–zirconia particle products at 250 °C with varying molar ratios

crystallite sizes of the ceria–zirconia particles were found at around 10.47, 8.96, 8.54, 5.2, and 7.03 nm on average when the ratios of ceria to zirconia in the starting materials were 4:1, 2:1, 1:1, 1:2, and 1:4, respectively.

It is well known that cerium oxide is the main substance in the three–way catalysis due to its high oxygen storage capacity. This property is associated with the ability of cerium oxide to undergo a rapid reduction–oxidation cycle (between Ce^{4+} and Ce^{3+}). When cerium ion is reduced to Ce^{3+}, the materials release oxygen, and when cerium ion is oxidized to Ce^{4+}, the materials store oxygen. Nevertheless, pure cerium oxide is not widely applicable due to its poor thermal stability and low oxygen storage capacity [6-7].

In this work, when the ceria particles obtained from hydrothermal treatment at a temperature of 250 °C with 2 h reaction time was submitted into the thermogravimeter device to measure its oxygen storage capacity, the amount of oxygen adsorbed was found at around 112.66 mmol–O_2/g of sample. By adding zirconia, the oxygen storage capacity of ceria and the thermal stability were significantly improved. The amounts of oxygen adsorption were 544.48, 652.39, 532.34, 614.71, and 447.38 mmol–O_2/g of sample when the ratios of ceria to zirconia in the starting materials were 4:1, 2:1, 1:1, 1:2, and 1:4, respectively. The specific surface area of these samples was around 86.73, 90.98, 92.03, 116.41, and 110.01 m^2/g of sample. It seemed that the values of the oxygen storage capacity were affected by the feed composition of the starting materials. This indicated that the surface area of the ceria–zirconia particles and its oxygen storage capacity were not strongly correlated. The value of the oxygen storage capacity increased with increasing amount of zirconia in the feed solution.

However, increasing zirconia content in the feed solution to over 50% did not significantly affect the oxygen storage capacity of the ceria–zirconia mixed oxides. On the contrary, the oxygen storage capacity value seemed to decrease to 447.38 mmol–O_2/g of sample when the mol% ratio of zirconia in the feed

solution was 80%. This indicated that the oxygen storage capacity was not dependent on the surface area of the materials, but they might have been controlled by the thermodynamic equilibrium of the redox reaction of the cerium oxide ions [5,37-42].

Cui et al. [40] investigated the influence of precipitation temperature on the properties of the ceria–zirconia solid solution composite. They reported that the increasing amount of zirconia in the ceria–zirconia solid solution composite did not improve the oxygen storage capacity. Furthermore, they pointed out that the lower amount of zirconia in the ceria–zirconia solid solution composite caused larger oxygen storage capacity. In addition, Cui et al. explained that the decline of textural properties and the shift of composition of the ceria–zirconia composites resulted in the decrease of oxygen storage capacity. Yin et al. [41] confirmed that the high oxygen storage capacity of the ceria–zirconia mixed oxides was associated with the addition of the zirconia substance. However, they also informed that due to the shift of the oxygen mobility in the ceria–zirconia mixed oxides, the higher amount of zirconia in the ceria–zirconia mixed oxides also resulted in ower oxygen storage capacity.

■ CONCLUSION

Ceria–zirconia mixed oxides particles were synthesized via hydrothermal technique at subcritical conditions, at temperatures of 200–300 °C and pressure of 10 MPa. At these conditions, water provides a favorable reaction medium for mixed metal oxides particles formation owing to the adjustability of the thermodynamics and transport properties via pressures and/or temperatures. The SEM images showed that the shapes or morphologies of the ceria–zirconia mixed oxides particles were spherical and spherical–like with a diameter of around 100 nm. The EDX spectrum showed that the signal corresponding to ceria (5 keV) and zirconia (2 keV) were strongly detected in the particle products. The XRD pattern revealed that the mixed metal oxide particles were comprised of cerium and zirconium oxide particles with cubic and monoclinic structures, respectively. Based on the results, this process can be considered as a feasible technique to produce metal oxide and mixed metal oxides from other types of metals.

■ ACKNOWLEDGMENTS

This research was supported by the Directorate General of Science, Technology and Higher Education, Ministry of Research, Technology and Higher Education of the Republic of Indonesia through the research grant "*Penelitian Dasar Unggulan Perguruan Tinggi*" 2018–2019 contract No. 925/PKS/ITS/2018 and 889/PKS/ITS/2019.

■ REFERENCES

[1] Trovarelli, A., 1996, Catalytic properties of ceria and CeO_2–containing materials, *Catal. Rev. Sci. Eng.*, 38 (4), 439–520.

[2] Montini, T., Melchionna, M., Monai, M., and Fornasiero, P., 2016, Fundamentals and catalytic applications of CeO_2–based materials, *Chem. Rev.*, 116 (10), 5987–6041.

[3] Li, C., Sun, Y., Djerdj, I., Voepel, P., Sack, C.C., Weller, T., Ellinghaus, R., Sann, J., Guo, Y., Smarsly, B.M., and Over, H., 2017, Shape–controlled CeO_2 nanoparticles: Stability and activity in the catalyzed HCl oxidation reaction, *ACS Catal.*, 7 (10), 6453–6463.

[4] Li, P., Chen, X., Li, Y., and Schwank, J.W., 2019, A review on oxygen storage capacity of CeO_2–based materials: Influence factors, measurement techniques, and applications in reactions related to catalytic automotive emissions control, *Catal. Today*, 327, 90–115.

[5] Trovarelli, A., and Fornasiero, P., 2013, *Catalysis by Ceria and Related Materials*, 2nd Ed., Imperial College Press, London, UK, p. 329, 666, 735.

[6] Ragurajan, D., Satgunam, M., and Golieskardi, M., 2014, The effect of cerium oxide addition on the properties and behavior of Y–TZP, *Int. Sch. Res. Notices*, 2014, 828197.

[7] Huang, H., Liu, J., Sun, P., Ye, S., and Liu, B., 2017, Effects of Mn–doped ceria oxygen–storage material on oxidation activity of diesel soot, *RSC Adv.*, 7 (12), 7406–7412.

[8] Manicone, P.F., Iommetti, P.R., and Raffaelli, L., 2007, An overview of zirconia ceramics: Basic properties and clinical applications, *J. Dent.*, 35 (11), 819–826.

[9] Zhang, Y., Malzbender, J., Mack, D.E., Jarligo, M.O., Cao, X., Li, Q., Vaßen, R., and Stöver, D., 2013, Mechanical properties of zirconia composite ceramics, *Ceram. Int.*, 39 (7), 7595–7603.

[10] Daou, E.E., 2014, The zirconia ceramic: Strengths and weaknesses, *Open Dent. J.*, 8, 33–42.

[11] Sen, N., and Isler, S., 2020, Microstructural, physical, and optical characterization of high–translucency zirconia ceramics, *J. Prosthet. Dent.*, 123 (5), 761–768.

[12] Kumar, A., Mansour, H.M., Friedman, A., and Blough, E.R., 2013, *Nanomedicine in Drug Delivery*, 1st Ed., CRC Press, Boca Raton, Florida, USA, p. 25.

[13] Hayashi, H., and Hakuta, Y., 2010, Hydrothermal synthesis of metal oxide nanoparticles in supercritical water, *Materials*, 3 (7), 3794–3817.

[14] Kaya, C., He, J.Y., Gu, X., and Butler, E.G., 2002, Nanostructured ceramic powders by hydrothermal synthesis and their applications, *Microporous Mesoporous Mater.*, 54 (1-2), 37–49.

[15] Machmudah, S., Prastuti, O.P., Widiyastuti, Winardi, S., Wahyudiono, Kanda, H., and Goto, M., 2016, Macroporous zirconia particles prepared by subcritical water in batch and flow processes, *Res. Chem. Intermed.*, 42 (6), 5367–5385.

[16] Pu, Y., Wang, J.X., Wang, D., Foster, N.R., and Chen, J.F., 2019, Subcritical water processing for nano pharmaceuticals, *Chem. Eng. Process. Process Intensif.*, 140, 36–42.

[17] Zhang, J., Kumagai, H., Yamamura, K., Ohara, S., Takami, S., Morikawa, A., Shinjoh, H., Kaneko, J., Adschiri, T., and Suda, A., 2011, Extra–low–temperature oxygen storage capacity of CeO_2 nanocrystals with cubic facets, *Nano Lett.*, 11 (2), 361–364.

[18] Demizu, A., Beppu, K., Hosokawa, S., Kato, K., Asakura, H., Teramura, K., and Tanaka, T., 2017, Oxygen storage property and chemical stability of $SrFe_{1-x}Ti_xO_{3-\delta}$ with robust perovskite structure, *J. Phys. Chem. C*, 121 (35), 19358–19364.

[19] Adschiri, T., and Yoko, A., 2018, Supercritical fluids for nanotechnology, *J. Supercrit. Fluids*, 134, 167–175.

[20] Adschiri, T., Kanazawa, K., and Arai, K., 1992, Rapid and continuous hydrothermal crystallization of metal oxide particles in supercritical water, *J. Am. Ceram. Soc.*, 75 (4), 1019–1022.

[21] Lane, M.K.M., and Zimmerman, J.B., 2019, Controlling metal oxide nanoparticle size and shape with supercritical fluid synthesis, *Green Chem.*, 21 (14), 3769–3781.

[22] Adschiri, T., Hakuta, Y., and Arai, K., 2000, Hydrothermal synthesis of metal oxide fine particles at supercritical conditions, *Ind. Eng. Chem. Res.*, 39 (12), 4901–4907.

[23] Zhang, Y., Zhang, L., Deng, J., Dai, H., and He, H., 2009, Controlled synthesis, characterization, and morphology–dependent reducibility of ceria–zirconia–yttria solid solutions with nanorod–like, microspherical, microbowknot–like, and micro–octahedral shapes, *Inorg. Chem.*, 48 (5), 2181–2192.

[24] Yang, Y., Wu, Q., Wang, M., Long, J., Mao, Z., and Chen, X., 2014, Hydrothermal synthesis of hydroxyapatite with different morphologies: Influence of supersaturation of the reaction system, *Cryst. Growth Des.*, 14 (9), 4864–4871.

[25] Hosokawa, M., Nogi, K., Naito, M., and Yokoyama, T., 2007, *Nanoparticle Technology Handbook,* 1st Ed., Elsevier, Amsterdam, Netherlands, p. 270–272.

[26] Machmudah, S., Zulhijah, R., Wahyudiono, Setyawan, H., Kanda, H., and Goto, M., 2015, Magnetite thin film on mild steel formed by hydrothermal electrolysis for corrosion prevention, *Chem. Eng. J.*, 268, 76–85.

[27] Tok, A.I.Y., Boey, F.Y.C., Dong, Z., and Sun, X.L., 2007, Hydrothermal synthesis of CeO_2 nano–particles, *J. Mater. Process. Technol.*, 190 (1-3), 217–222.

[28] Kaminski, P., Ziolek, M., and van Bokhoven, J.A., 2017, Mesoporous cerium–zirconium oxides modified with gold and copper – Synthesis, characterization and performance in selective oxidation of glycerol, *RSC Adv.*, 7 (13), 7801–7819.

[29] Parimi, D., Sundararajan, V., Sadak, O., Gunasekaran, S., Mohideen, S.S., and Sundaramurthy, A., 2019, Synthesis of positively and negatively charged CeO_2 nanoparticles: Investigation of the role of surface charge on growth and development of *Drosophila melanogaster*, *ACS Omega*, 4 (1), 104−113.

[30] Phokha, S., Pinitsoontorn, S., Chirawatkul, P., Poo–arporn, Y., and Maensiri, S., 2012, Synthesis, characterization, and magnetic properties of monodisperse CeO_2 nanospheres prepared by PVP–assisted hydrothermal method, *Nanoscale Res. Lett.*, 7, 425.

[31] Alammar, T., Noei, H., Wang, Y., Grünert, W., and Mudring, A.V., 2015, Ionic liquid–assisted sonochemical preparation of CeO_2 nanoparticles for CO oxidation, *ACS Sustainable Chem. Eng.*, 3 (1), 42–54.

[32] Zhang, X., Wang, Q., Zhang, J., Wang, J., Guo, M., Chen, S., Li, C., Hu, C., and Xie, Y., 2015, One step hydrothermal synthesis of CeO_2–ZrO_2 nanocomposites and investigation of the morphological evolution, *RSC Adv.*, 5 (109), 89976–89984.

[33] Darr, J.A., Zhang, J., Makwana, N.M., and Weng, X., 2017, Continuous hydrothermal synthesis of inorganic nanoparticles: Applications and future directions, *Chem. Rev.*, 117 (17), 11125–11238.

[34] Devaiah, D., Reddy, L.H., Park, S.E., and Reddy, B.M., 2018, Ceria–zirconia mixed oxides: Synthetic methods and applications, *Catal. Rev. Sci. Eng.*, 60 (2), 177−277.

[35] Prasad, D.H., Park, S.Y., Ji, H., Kim, H.R., Son, J.W., Kim, B.K., Lee, H.W., and Lee, J.H., 2012, Effect of steam content on nickel nano–particle sintering and methane reforming activity of Ni–CZO anode cermets for internal reforming SOFCs, *Appl. Catal.*, *A*, 411-412, 160–169.

[36] Zaytseva, Y.A., Panchenko, V.N., Simonov, M.N., Shutilov, A.A., Zenkovets, Renz, M., Simakova, I.L., and Parmon, V.N., 2013, Effect of gas atmosphere on catalytic behaviour of zirconia, ceria and ceria–zirconia catalysts in valeric acid ketonization, *Top. Catal.*, 56 (9), 846–855.

[37] Uzunoglu, A., Zhang, H., Andreescu, S., and Stanciu, L.A., 2015, CeO_2–MO_x (M: Zr, Ti, Cu) mixed metal oxides with enhanced oxygen storage capacity, *J. Mater. Sci.*, 50 (10), 3750–3762.

[38] Hirano, M., and Suda, A., 2003, Oxygen storage capacity, specific surface area, and pore–size distribution of ceria–zirconia solid solutions directly formed by thermal hydrolysis, *J. Am. Ceram. Soc.*, 86 (12), 2209–2211.

[39] Suda, A., Yamamura, K., Hideo, S., Ukyo, Y., Tanabe, T., Nagai, Y., and Sugiura, M., 2004, Effect of the amount of Pt loading on the oxygen storage capacity of ceria–zirconia solid solution, *J. Jpn. Soc. Powder Powder Metall.*, 51 (11), 815–820.

[40] Cui, Y., Fang, R., Shang, H., Shi, Z., Gong, M., and Chen, Y., 2015, The influence of precipitation temperature on the properties of ceria–zirconia solid solution composites, *J. Alloys Compd.*, 628, 213–221.

[41] Yin, K., Davis, R.J., Mahamulkar, S., Jones, C.W., Agrawal, P., Shibata, H., and Malek, A., 2017, Catalytic oxidation of solid carbon and carbon monoxide over cerium–zirconium mixed oxides, *AIChE J.*, 63 (2), 725–738.

[42] Wang, L., Chen, S., Hei, J., Gao, R., Liu, L., Su, L., Li, G., and Chen, Z., 2020, Ultrafine, high−loading and oxygen−deficient cerium oxide embedded on mesoporous carbon nanosheets for superior lithium−oxygen batteries, *Nano Energy*, 71, 104570.